Numerical modelling of downward progressive failure in sensitive clays; the case of the 1976 landslide at Saint-Fabien, Québec

Tremblay-Auger, F., Locat, A., & Leroueil, S.
Département de génie civil et de génie des eaux – Université Laval, Québec, Québec, Canada
Demers, D.
Ministère des transports du Québec, Québec, Canada

ABSTRACT
The Saint-Fabien landslide occurred in December 1976, 270 km north-east of Quebec City, Canada. Passive and active failure zones were observed in the debris, indicating a downward progressive failure mechanism, unusual in Eastern Canadian clays. Conventional stability analysis was performed at the site and a factor of safety of 1.43 was obtained. This means that limit equilibrium analysis cannot explain the formation of the failure surface observed at Saint-Fabien. The initiation and the propagation of the failure were analysed through 1D numerical modelling using the concept of progressive failure. The methodology consists of two steps: first the calculation of the initial stresses in the slope with the finite element software PLAXIS 2D and second the modelling of progressive failure initiation and propagation with the finite element code BIFURC, developed at the Norwegian Geotechnical Institute.

RÉSUMÉ
Le glissement de Saint-Fabien s'est produit le 16 Décembre 1976, 270 km au nord-est de la ville de Québec. Des zones passive et active ont été observées dans les débris, indiquant un mouvement translationnel progressif vers le bas, peu commun dans les argiles de l'est du Canada. L'analyse de stabilité conventionnelle a donné un coefficient de sécurité de 1.43. La méthode à l'équilibre limite ne permet donc pas d'expliquer la formation de la surface de rupture observée à Saint-Fabien. L'initiation et la propagation de la rupture ont été analysées avec la modélisation numérique en 1D en utilisant le concept de rupture progressive. Les deux étapes de cette analyse sont : premièrement le calcul des contraintes initiales dans la pente avec le logiciel par éléments finis PLAXIS 2D et deuxièmement la modélisation de la propagation de la rupture progressive avec le code d'éléments finis BIFURC, développé à l'Institut Norvégienne de Géotechnique.

1 INTRODUCTION

On December 16th, 1976, a landslide occurred near the municipality of Saint-Fabien, 270 km northeast of Quebec City, Canada, along the Road 132. This landslide was first studied by the Quebec Ministry of Transportation (MTQ) during the following year.

Particular features of the landslide are its almost horizontal ground surface and failure surface. The presence of active and passive failure zones in the debris was also noted, indicating a downward progressive failure mechanism, unusual in Eastern Canadian clays (Locat and al. 2011). University Laval was interested in this unique event and decided to study the landslide in detail in 2005, in collaboration with the MTQ (Levasseur, 2006), and later in 2017-2018 to complete the analysis.

This paper presents a brief description of the event, the geotechnical properties, general topography and stratigraphy and the hydrogeological conditions in the landslide area. The conventional stability analysis is then presented, followed by the analysis considering progressive failure. The calculation of the initial stresses is described first and then the effects of the possible triggers on those initials stresses in the slope are analysed. The results of the numerical modelling of progressive failure regarding initiation, propagation and global failure are then explained.

2 DESCRIPTION OF THE EVENT

The 1976 landslide at Saint-Fabien is delineated by the dashed line on Figure 1 showing a 1977 aerial photograph of the site. It is 600 m wide (along the road) and 300 m long. Subsidence of the ground south of the road and a heaving zone north were observed. The failure surface progressed from south to north with a downward propagation. It came out of the soil north of the road in a small ditch of approximately 0.75 m on the west side and in the exploited peat bog deposit (B) on the east side. Compression fissures can be seen in the debris, north of the road (see Figure 1). The landslide took place in a rocky valley filled with glaciomarine clays covered by peat bogs. In the middle of the valley, just north of Road 132, there was a continuous exploitation of the peat bog (see Figure 1). Road 132 and the Canadian National Railway (CN) follow the valley and were damaged and displaced by the landslide movement. The CN was therefore forced to stop its operations in this sector for some time.

At the time of the landslide, the MTQ was working along Road 132. Works near the landslide area started on October 6th, 1976 and were supposed to be completed before November 8th, 1977. The objective was to raise the roadway by 0.5 m to 1 m and to widen it by approximately 3 m between stations 252+00 and 329+00 (Levasseur, 2006).

Roadworks East of station 302+00 (in the middle of the landslide area) were completed on November 9th, 1976 (Figure 1). West of station 302+00 (Figure 1), roadworks started on October 7th, 1976. On December 15th and 16th, the workers were placing the fifth and last layer of embankments fill. On December 16th, they were progressing from the West toward the East. When the movement suddenly started, around 11 am, they were working near station 289+00 (Figure 1). Following the event, the CN decided to sue the MTQ for the railway damages and the loss of money associated with the stoppage of the operations caused by the landslide. Records from this lawsuit enable us to obtain several testimonies of the event from eyewitnesses and to reconstitute the sequence of the movements. In summary, witnesses saw the first movement start in the northeast area, near the peat bogs (B), in the section where the roadworks had been completed more than five weeks earlier. They then saw the landslide propagates toward the west. For further description of the witnesses testimonies, please refer to (Tremblay-Auger et al. 2018).

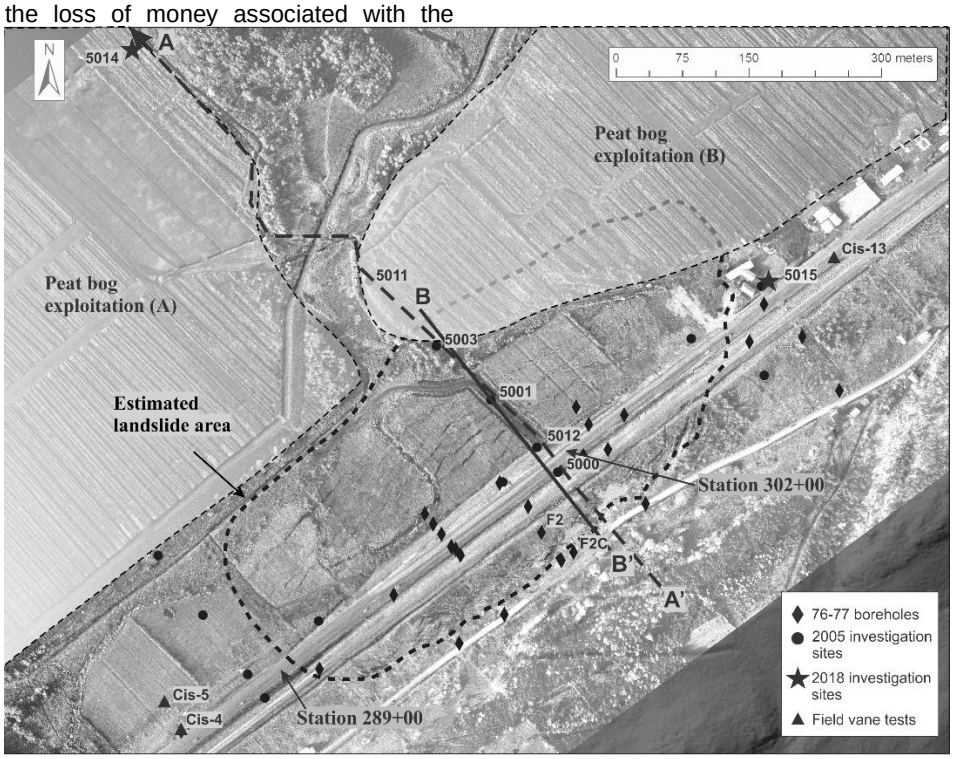

Figure 1. Location of the boreholes performed in 1976 and 1977 and the investigation works done in 2005 and 2018. Cross sections A-A' and B-B' are shown in the middle of the landslide. Location of stations 289+00 and 302+00 for the roadworks, and the peat bogs exploitations.

3 GEOTECHNICAL INVESTIGATIONS: SITE AND SOIL CHARACTERISTICS

The geotechnical investigation at the site was performed in three phases: 1976-1977, 2005 and 2018. In all cases, the MTQ was in charge of the investigation. The topography before the landslide in 1976 and after in 1977 was obtained from photogrammetry. The precision of this method is between 0.5 m and 1 m at best. A Lidar survey of the area was also performed in 2013 with a precision of 0.25 m. The first phase of investigation included 29 boreholes, 26 field vane test profiles and the installation of 18 piezometers. Selected boreholes performed in 1976 and 1977 are located by black diamonds on Figure 1. In the second phase, two boreholes and two field vane test profiles were performed and three additional piezometers were installed. There were also 14 piezocone penetration tests with pore pressure measurements (CPTUs) that were performed. Figure 1 shows the CPTUs performed in 2005 with black dots. The 2005 piezometers were installed at locations 5000, 5001 and 5011 and the field vane tests and boreholes were carried out at locations 5000 and 5001. For the third phase, the objective was to have a complete geotechnical profile in the intact deposit, outside the landslide limit. An additional borehole, CPTU and field vane tests were performed and piezometers were installed at location 5015, just east of the landslide limit. Other piezometers were also installed at location 5014, near the middle of the valley and a CPTU was also performed at this site. The 2 new sites 5014 and 5015 performed in 2018 are represented by stars on Figure 1. A gravity survey was also carried out through the valley to determine the depth of the bedrock and its morphology (Cross section A on Figure 1)

3.1 Topography, stratigraphy and hydrogeological conditions

Figure 2 presents cross section B (see location on Figure 1). The site stratigraphy in the central part of the landslide was interpreted using information from 4 boreholes (5001, 5000, F-2 and F-2C, shown on Figure 1) and 4 CPTUs (5003, 5001, 5012 and 5000, also shown on Figure 1).

The CPTUs were used to determine the depth of the till layer, which was associated with the maximum tip resistance. The stratigraphy of the site consists of a 3 m to 5 m peat layer and/or a 5 m to 7 m road/rail embankment of sand and gravel, underlain by a thick layer of soft silty clay, which will be described in the next section. The clay deposit is underlain by about 3 m thick of till resting on bedrock. On Figure 2, it can be noticed that the bedrock surface below the landslide area dips in a northerly direction.

The dotted line on Figure 2 shows the failure surface as estimated from CPTU profiles. The interpreted failure surface is marked with an "x" on cross section B (Figure 2) at locations 5001, 5012 and 5000 at elevations of 78, 80.5 m and 78 m respectively. Those are approximately at a depth of 13 m below the initial ground surface.

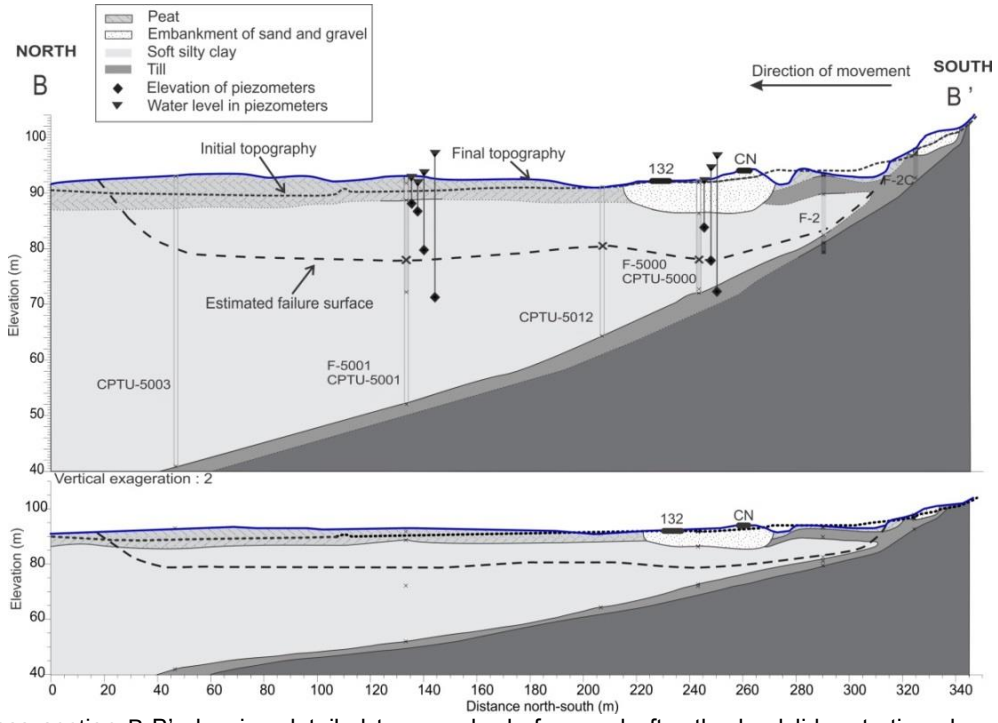

Figure 2. Cross section B-B' showing detailed topography before and after the landslide, stratigraphy, water level in piezometers and failure surface. The upper cross section is depicted with 2X vertical exaggeration, and the lower cross section is depicted with no vertical exaggeration.

The cross section B (Figure 2) also presents the water levels in piezometers at locations 5000 and 5001. An upward flow with a gradient of about 0.41 is noted in the clay deposit at location 5001, and of about 0.39 in the till at location 5000. At location 5015 (not on the cross section B, see its location on Figure 1) they indicate an upward flow with a gradient of 0.50. Those gradients are probably caused by water pressure coming from the till outcropping at the south limit of the valley (see Figure 2). Actually, the piezometer 5011 that is farther from the side of the valley and north of the landslide limit (see Figure 1) gives a much lower value of 0.05 for the gradient, which is almost hydrostatic conditions.

3.2 Geotechnical properties of the clay deposit

The deposit involved in the landslide is a soft clay and silt with traces of sand and gravel with a high sensitivity. The geotechnical properties of the clay along the potential failure surface (elevation of 81 m) are presented at the sites 5015 and 5001. Site 5015 is outside the landslide limit, in the intact material, and close to the road 132 (see Figure 1). Site 5001 is 100 m further from the road, in the middle of the landslide area in the debris (see Figure 1). Those properties are presented in Table 1.

Table 1. Geotechnical properties at sites 5015 and 5001 at the elevation of the failure surface

Properties (%)	Site 5015	Site 5001
Water content	40 %	50 %
Liquid limit	24 %	28 %
Plastic limit	18 %	20 %
Plasticity index	6	8
Liquidity index	3	4
Sensitivity (Su/Sur)	61	57
CPTU's corrected tip resistance (q_t)	440 kPa	260 kPa
Undrained shear strength (Field vane test Su)	17 kPa (Cis-13)	7 kPa
OCR	1.5	1.0
Hydraulic gradient	0.50	0.41

Laboratory testing was carried out including grain-size distributions, water contents (w), consistency limits (plastic limit, w_p, and liquid limit, w_L) and sensitivity (St)

calculated from the intact (Su) and remoulded (Su_r) shear strengths measured with the Swedish fall cone.

What is important to note about those properties is that further we get from the road, the more normally consolidated the deposit gets, OCR value is decreasing from 1.5 close to the road to 1.0 some tens of meters north of the road. In addition, the deposit also gets softer; Su is decreasing from 17 kPa close to the road to 7 kPa some tens of meters further. For complete description of the geotechnical profile at location 5001, please refer to (Tremblay-Auger et al. 2018).

4 CONVENTIONAL STABILITY ANALYSIS

The stability of a 5 m embankment, which is the thickness of the embankment measured in the field directly after the event, was estimated with the limit equilibrium analysis using the software GeoStudio 2012 (GeoSlope, 2012). The model used a cross section of the landslide area showing approximately half the valley on a distance of 420 m with the embankment on the right side. A steady-state seepage analysis was first done and then a SLOPE/W stability analysis was performed. Hydraulic conditions as observed in the piezometers at locations 5011, 5001 and 5000 were input in the model. The analysis was performed with undrained conditions for the clay where the properties are governed by the profile of the undrained shear strength obtained from the field vane test Cis-13, near the road (see location on Figure 1). The properties of the clay, embankment and peat layers used in the modelling are listed in Table 2. Bjerrum's correction factor was not applied, as the plasticity index is smaller than 20.

Table 2. Properties of the different layers of soil used for the limit equilibrium analysis in GeoStudio

Material	Unit Weight (kN/m^3)	Cohesion or Su (kPa)	Φ (°)
Clay	17	From 15 to 27 (Su from Cis-13)	-
Embankment	19	1	30
Peat	11	2	23

The factor of safety of the most critical failure surface is 1.43, which is well above unity. This indicates that the ground near the road was stable when the construction works were performed. The same analysis was done with an additional 1 m of embankment to simulate the roadworks. The factor of safety was minimally affected by this and a value of 1.19 was obtained. This is consistent with the fact that no circular failure surface was observed near the road by the witnesses. This indicates that the roadworks might not have initiated a circular failure under the embankment.

5 PRELIMINARY ANALYSIS CONSIDERING PROGRESSIVE FAILURE

The morphology of the Saint-Fabien landslide previously described shows similarities with downward translational landslides as described by Bernander et al. (2016) and Locat and al. (2011). Those landslides often take place in slightly inclined slopes of nearly normally consolidated sensitive clay. They are often caused by human activity uphill such as fill loading or pile driving that can increase earth pressures and lead to the formation of a failure surface progressing downhill and generating a passive failure of the slope. The typical morphology of those movements consists of an active subsidence zone uphill and a passive heave zone downhill. Between those two areas, there is a zone of soil that experiences mostly translational movement.

Locat and al. (2013) presented a numerical method that uses the concept of progressive failure, as described by Bernander (2008, 2016), to model spreads in sensitive clays (Locat and al. 2013, 2015). The hypothesis in these cases is that failure is initiated at the bottom of a slope and can propagate upslope, as presumably occurred for the 1994 Saint-Monique spread (Locat and al. 2015). The methodology used by Locat and al. (2013) is used here to study the Saint-Fabien landslide as a downward progressive failure. In this case, the hypothesis is that the failure is initiated at the top of the slope and can propagate downslope. The methodology consists of two steps: (i) calculation of the initial stresses in the slope with the finite element software PLAXIS 2D (PLAXIS, 2018); and (ii) modelling of the initiation and the propagation of the progressive failure with the 1D finite element code BIFURC (Jostad and Andersen, 2002, see also Locat et al. 2013 and 2015).

5.1 Calculation of the initial stresses with PLAXIS 2D

For the first part of the numerical analysis, a model including the three soil layers (peat, clay and till) and extending to approximately half of the valley where the landslide occurred was created in PLAXIS. The geometry of the model is presented on Figure 3. On the same figure, the 5 CPTUs and piezometer sites, 5014, 5011, 5001, 5015 and 5000, are located. The "hardening soil model" in PLAXIS was used for the three different soil layers and the embankment of sand and gravel. The soil properties of the clay layer are presented in Table 3. In this case, the reference stress p_{ref} is 100 kPa. It was considered that the entire deposit is essentially normally consolidated, except near the road where the deposit is slightly overconsolidated, as explained previously. An OCR value of 1.0 was therefore assumed for the entire deposit, as was a p_{ref} value of 100 kPa and a $\sigma'_p{}^{ref}$ value of 100 kPa. The elevation of the water table was set at the elevation of the ground surface, and a uniform head water elevation of 104 m was assumed over the entire thickness of the till layer at the right boundary of the model. A free seepage boundary was applied at the left boundary of the model and an impermeable boundary was set at the bottom of the till layer to recreate contact with the bedrock. The initial stresses in the deposit were calculated with gravity loading (PLAXIS, 2018). To verify the accuracy of the model, the calculated pore pressures and initial vertical effective stresses were compared to the

data collected in the field at sites 5014, 5011, 5001, 5015 and 5000 to be certain that the results were similar. The total horizontal stresses (σ_{x0}) and shear stresses (τ_0) along a potential failure surface were then extracted from the model. The elevation of this potential failure surface was set at an elevation of 81 m, which is representative of what was observed at the site. Figure 4 shows those initial stresses ($\tau_0(x)$ and $\sigma_{x0}(x)$) along this potential failure surface (black dashed lines on Figure 4b and c). It can be observed that both the shear stresses and the total horizontal stresses are constant in the horizontal deposit and then start to increase near the road embankment. The shear stress is around 0 kPa between -280 m and 100 m (see Figure 4b). After this point, it starts to increase slowly up to a value of 2 kPa at 200 m. Then, it increases rapidly due to the surcharge caused by the embankment, reaching a maximum value of 14 kPa directly below the edge of the embankment. The shear stress then decreases below the embankment, at a distance of 240 m. The total horizontal stress is around 115 kPa between -280 m and 100 m (see Figure 4c). The shear stress increases with the increase of the inclination of the slope, up to 175 kPa, below the embankment, at a distance of 240 m.

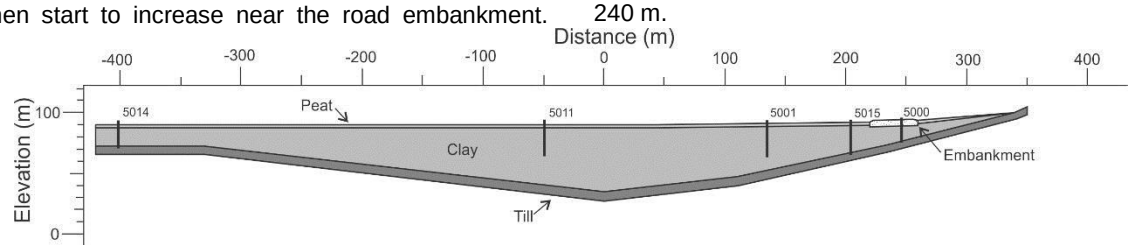

Figure 3. Geometry of the model used in PLAXIS

Table 3. Clay properties used in PLAXIS

Parameters	Symbol	Clay
Secant stiffness for primary deviatoric loading (kPa)	$E_{50}^{ref} \approx E_{oed}^{ref}$	9000
Tangent oedometer stiffness (kPa)	$E_{oed}^{ref} \approx 90\sigma'^{ref}_{p}$	9000
Unloading / Reloading stiffness (kPa)	$E_{ur}^{ref} \approx 3E_{50}^{ref}$	27 000
Soil unit weight (kN/m^3)	γ	17
Cohesion (kPa)	c′	7.5
Friction angle (°)	ϕ′	30
Poisson's ratio	ν′	0.25
Horizontal and vertical hydraulic conductivity (m/s)	k_x and k_y	10^{-9}

5.2 Modelling the effect of the earth works and the peat bogs exploitation in the landslide area with Plaxis 2D

As described previously, two important actions were taking place at the time of the landslide. There was continuous exploitation of the peat bogs deposit close to the landslide and the MTQ was working along Road 132. The effect of those two events on the initial stresses was modelled with PLAXIS 2D and is presented in Figures 4b and c. Field vane test Cis-5 (see location on Figure 1) represents the conditions of the deposit well, far from the road. At an elevation of 81 m, which is the assigned elevation of the failure surface in the PLAXIS 2D model, the peak shear strength of the soil is around 10 kPa and is delineated on Figure 4 by τ_{p1} (x). The peak shear strength of the soil near the embankment is defined by Cis-13 (see τ_{p2} (x) on Figure 4) and the value is around 17 kPa at an elevation of 81 m.

As the information regarding the earth works and peat exploitation is not accurately known, the results of the analyses are only schematic in nature. The exploitation of the peat was modelled by removing 2 m of peat at the location of peat bog exploitation (B), observable on Figure 1. It can be seen on Figure 4b that this excavation has the effect of decreasing and then increasing the shear stress by about 7 kPa in the soil and also decreasing the total horizontal stress by 10 kPa (Figure 4c). From this analysis, it seems that the exploitation of the peat did not generate shear stress larger than the peak shear strength of the soil.

The roadworks were modelled by raising the embankment by 1 m over the width of the road embankment (10 m). Due to the lack of precise information, this value is an approximate, and is probably lower than the real value, but was still used to get an idea of the influence of the roadworks. This additional weight had the effect of increasing the shear stress and the horizontal stress near the road (see Figure 4b and c). The shear stress and the total horizontal stress are now reaching maximum values of 17 kPa and 180 kPa, respectively, instead of 14 kPa and 175 kPa. The additional 1 m of embankment fills has the effect of increasing the shear stress close to τ_{p1} (x) at point A. At a distance of 220 m, where the maximum value of shear stress is mobilized (see Figure 4b), it can be noted that the roadworks have the effect of increasing the shear stress to a maximum value equal to τ_{p2} (x). This could have initiated a progressive failure.

It is important to note that, given the results of the modelling, the exploitation of the peat downslope has no influence on the stresses near the road and similarly the roadworks do not have any effect on the stresses downslope.

5.3 Modelling progressive failure with BIFURC

For the second part of the numerical analysis, which is the modelling of the initiation and the propagation of the failure surface with BIFURC, the initial stresses mentioned earlier were extracted from a distance of -290 m to a distance of 210 m (point A) and input in BIFURC. Point A, on Figure 4, was chosen as it refers to the point on the failure surface that is at an angle of 60° from the edge of the embankment. This point is considered the

location of the initiation of the failure in BIFURC's model. Only the part of the deposit north of point A (Figure 4) was considered and was assumed homogeneous. The initial stresses along the potential failure surface extracted from the modelling with PLAXIS and shown on Figure 4b and c were input as initial parameters in BIFURC. The shear stresses (τ_0) were taken as presented on Figure 4b. The average total horizontal stress above the failure surface or shear band was considered in BIFURC, which is ($\sigma_{x0}/2$). The other parameters required in the modelling are listed in Table 4. For this part of the modelling, parameters were taken from the geotechnical profile 5001, which is more representative of the entire deposit (see Table 1). For the soil above the shear band, the elastic shear stiffness modulus (G^e) refers to the peak shear strength over the deformation at peak shear strength (τ_p/γ_p = 10/0.01 = 1000 kPa). As explained previously, the peak shear strength is obtained from the field vane test Cis-5 in the intact deposit and is around 10 kPa and the deformation at peak is usually between 0.6 and 1.2 % in eastern Canadian clays (Leroueil, 1997), so a value of 1% was considered. The stiffness modulus in compression and extension (E_{el}) is about three times G^e and should also be around $90\sigma'_p$ according to Leroueil and al. (1983). Also, the deposit is nearly normally consolidated. Therefore, the preconsolidation pressure at the depth of the failure surface was taken from profile 5001 and is around 37 kPa (E_{el} = $90\sigma'_p$ = 90*37 = 3330 kPa). The shear band thickness (t) is an unknown parameter and was varied between 0.1 m and 1.0 m.

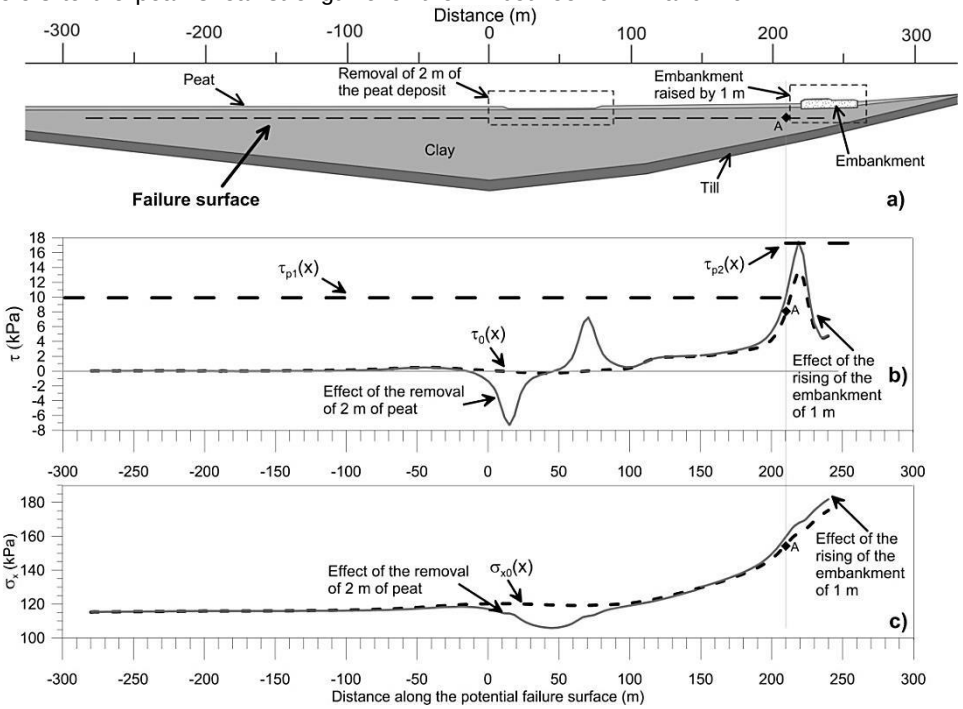

Figure 4. Initial stresses along the potential failure surface and the combined effect of the removal of 2m of peat and the raising of the embankment by 1 m

Table 4. Parameters used in the modelling of progressive failure with BIFURC

Parameters	Values
Truss element	
Elastic shear stiffness modulus (Ge)	1000 kPa
Undrained stiffness modulus in compression and extension (Eel)	3330 kPa
Interface element	
Peak shear strength (τ_p)	10 kPa
Shear band thickness (t)	(0.1-1.0) m
Total displacement at the peak shear strength (δ_p)	(0.001-0.01) m
Total displacement when the large deformation shear strength is first reached (δ_{ld})	(0.03-0.3) m
Large deformation shear strength (τ_{ld})	(0.7-1.5) kPa

The brittleness of the soil, which refers to the rapidity at which the shear strength goes from the peak to the large deformation, was varied. The total displacement at the peak shear strength ($\delta_p = \gamma_p t$) and the total displacement when the large deformation shear strength is reached ($\delta_{ld} = \gamma_{ld} t$) are both dependent on the thickness of the shear band. A value of 30% for the deformation at large strains (γ_{ld}) was considered.

The influence of the sensitivity of the soil was analysed by varying the large deformation strength (τ_{ld}), which is also an unknown parameter. Varying values between 0.7 kPa and 1.5 kPa were used, which is close to the values of Sur measured with the Swedish fall cone.

With this simulation, two conditions were established to explain the Saint-Fabien landslide; 1) the propagation distance of the failure surface needs to be ≥200 m; and 2) a passive failure needs to occur. These two aspects are discussed in the next two sections.

5.3.1 Propagation

Figure 5 presents the maximum propagation distance at the end of the progressive failure as a function of the large deformation shear strength for the different shear band thicknesses and large deformation shear strength considered in the analysis. For each simulation, the propagation distance at which the progressive failure stopped was noted. It can be seen on Figure 5 that at a large deformation shear strength of 1.5 kPa and over, the propagation distance is the same for all the different thicknesses of the shear band. It can be noted that the propagation distance of the failure surface is very sensitive to the value of the large deformation shear strength. At the Saint-Fabien landslide, a distance of propagation of approximately 200 m was observed in the field, as noted on Figure 5 by the dashed black line. It can be observed that only the simulations giving failure propagation distances above this limit can explain what was observed on the field.

5.3.2 Global failure

For a passive failure to occur and explain the Saint-Fabien landslide, the passive strength (σ_{Pas}) of the soil above the failure surface has to be reached. The passive strength of the soil is the maximum strength that the soil above the shear zone can be subjected to before reaching passive failure.

The passive strength varies from a value of 116 kPa down to a value of 80 kPa between distances of 0 to 150 m, and stays constant at 80 kPa between 150 m and 350 m, where the peat bog was exploited, and then increases to 85 kPa in the horizontal part of the deposit. These passive earth pressures are presented in Figure 6 c).

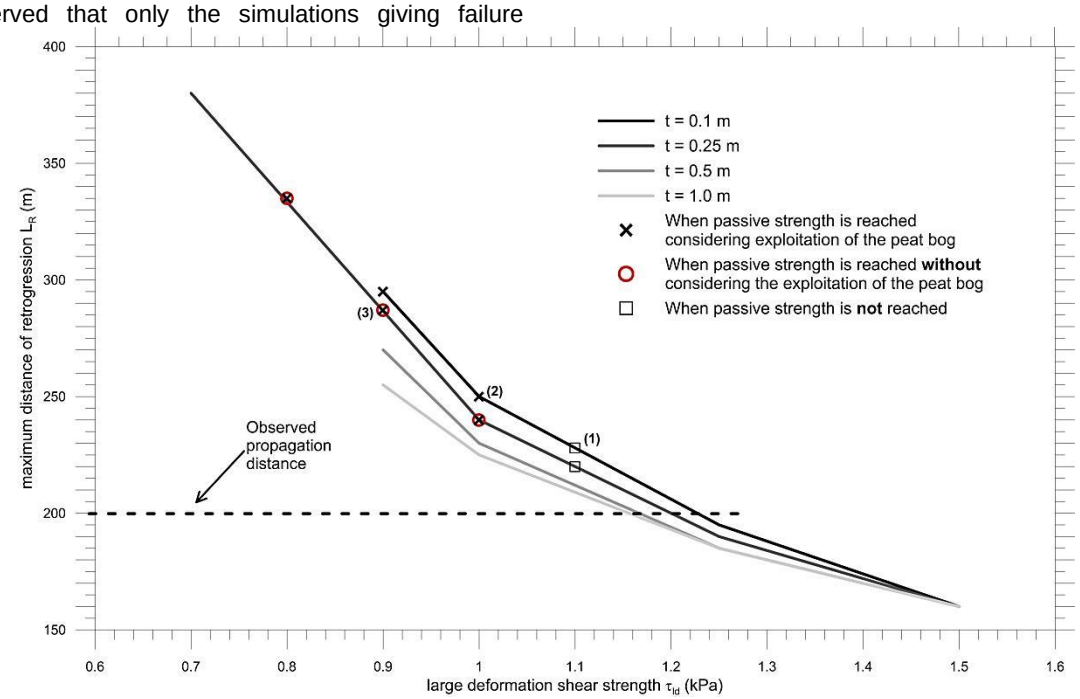

Figure 5. Maximum propagation distance as a function of the large deformation shear strength for different thicknesses of the shear band

Three situations were considered for this analysis and results are shown on Figure 5. The points represented by an "x" are simulations where the passive strength was reached only when considering the exploitation of the peat bog. Red circles represent the cases when the passive strength was reached without any consideration of the exploitation of the peat bog and the squares show situations when the passive strength is never reached, despite peat bog exploitation.

Figure 6 presents specific examples (3) from the summary in Figure 5, in which the passive strength is reached without the necessity of considering the exploitation of the peat bog. Figure 6a presents the modelled initial ground surface used in BIFURC. The shape of the ground surface after the landslide is depicted and the propagation distance observed in the field is also noted. Figure 6b presents the evolution of the shear stress along the potential failure surface at different increments or times during the simulation. Time 0 represents the conditions of initial shear stresses in the deposit before the landslide, time 1 is the state of the shear stress at the initiation of progressive failure and time 2 is the state of shear stresses at the end of the failure propagation. The shear band propagates to a distance of 250 m, which is 50 m further than what was observed in the field. Figure 6c presents the evolution of the average horizontal stress above the failure surface for the same three times. On this graph the passive strength (σ_{Pas}) considering exploitation of the peat is depicted with the bold dashed line (in blue it is without considering the exploitation of the peat). It can be seen that the horizontal stress at the end of propagation (time 2) reaches the passive strength of the soil without considering the exploitation of the peat, generating passive failure. These combinations of parameters therefore seem to explain the

passive failure observed at Saint-Fabien, as the two conditions are respected (failure propagation and passive failure).

In Figure 6c the state of the stresses at an intermediate time (time *) shows that the passive strength of the soil is reached when considering the exploitation of the peat, generating passive failure at a propagation distance of about 200 m, which also respects both conditions mentioned above.

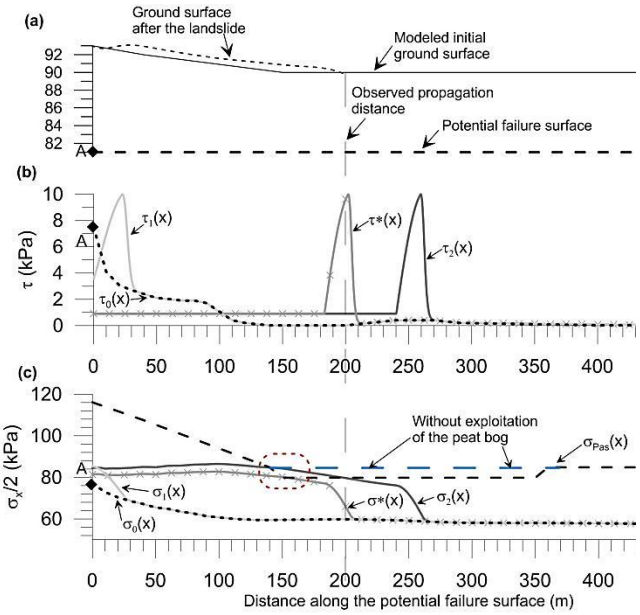

Figure 6. Results of progressive failure with t = 0.25 m and τ_{ld} = 0.9 kPa.

6 CONCLUSION

The Saint-Fabien landslide that occurred in 1976 has been studied in detail by the MTQ and University Laval. At the time of the event the MTQ was working along road 132 near the landslide area and there was also continuous exploitation of a peat layer downslope. Conventional stability analysis was performed near the road, and a factor of safety well above unity was obtained. The concept of progressive failure, as described by Bernander (2008, 2016) and Locat and al. (2011), is considered to explain the extent of the observed landslide. As passive and active zones were noted in the field, the Saint-Fabien landslide was studied as a downward progressive failure. Results regarding the raising of the embankment show that it brought the shear stress close to the shear strength of the soil and could have initiated a progressive failure. The analysis shows that exploitation of the peat decreases substantially the average horizontal stress downslope, which could have helped created the conditions for a passive failure to take place. Results from the modelling with BIFURC show that the concept of progressive failure is able to explain the extent of the landslide observed at Saint-Fabien with parameter values based on what was measured in situ.

7 ACKNOWLEDGMENTS

The authors would like to acknowledge the MTQ for the permission for using their data, and the Plan d'action 2013-2020 sur les changements climatiques and the Fond Vert 2013-2020 for their financial contribution of 494 366,35 $. The Natural Sciences and Engineering Research Council of Canada is also recognized for its financial support.

8 REFERENCES

Bernander, S. 2008. Down-hill progressive landslides in soft clays, triggering disturbance agents, slide propagation over horizontal or gently sloping ground, sensitivity related to geometry. *Research Report.* Department of Civil and Mining Engineering, Luleå University of Technology, Luleå, Sweden.

Bernander, S., Kullingsjö, A., Gylland, A.S., Bengtsson, P.E., Knutsson, S., Push, R., Olofsoon, J. and Elfgren, L. 2016. Downhill progressive landslides in long natural slopes: triggering agents and landslide phases modelled with a finite difference method, *Canadian Geotechnical Journal*. 53: 1565-1582.

GeoStudio. 2012. Stability Modelling with GeoStudio. *GEO-SLOPE International* Ltd, Calgary, Canada.

Jostad, H.P., and Andresen, L. 2002. Capacity analysis of anisotropic and strain-softening clays. In *Proceedings of the NUMOG VIII,* Rome, Italy, pp. 469–474.

Leroueil, S., Tavenas, F., and Le Bihan, J.-P. 1983. Propriétés caractéristiques des argiles de l'est du Canada. *Canadian Geotechnical Journal*, 20(4): 681–705. doi:10.1139/t83-076.

Leroueil S. 1997. Geotechnical characteristics of eastern Canada clays, *Workshop on soft clays*, Yokosuka, Japan.

Levasseur, P.-P. 2006. Compilation des données existantes sur le glissement de Saint-Fabien du 16 décembre 1976, *Rapport d'avancement*, Service de géotechnique et de la géologie, ministère des Transports du Québec.

Locat, A., Leroueil, S., Bernander, S., Demers, D., Jostad, H.P., and Ouehb, L. 2011. Progressive failures in eastern Canadian and Scandinavian sensitive clays. *Canadian Geotechnical Journal*, 48(11): 1696–1712.

Locat, A., Jostad, H.P., and Leroueil, S. 2013. Numerical modeling of progressive failure and its implications for spreads in sensitive clays. *Canadian Geotechnical Journal*, 50(9): 961–978.

Locat A., Leroueil, S., Fortin, A., Demers, D. and Jostad, H.P. 2015. The 1994 landslide at Saint-Monique, Quebec: geotechnical investigation *and application of progressive failure analysis. Canadian Geotechnical Journal*, 52: 490-504.

PLAXIS. 2018. PLAXIS 2D 2018. PLAXIS bv. Delft, the Netherlands.

Tremblay-Auger, F., Levasseur, P-P., Demers, D., Leroueil, S. & Locat, A. 2018. The 1976 landslide at Saint-Fabien, Québec. *Proceedings of the 7th Canadian Geohazards Conference*, Canmore, Canada. 7 p.